NACA TN 3822

NATIONAL ADVISORY COMMITTEE FOR AERONAUTICS

TECHNICAL NOTE 3822

SOME MEASUREMENTS OF AERODYNAMIC FORCES AND MOMENTS AT SUBSONIC SPEEDS ON A WING-TANK CONFIGURATION OSCILLATING IN PITCH ABOUT THE WING MIDCHORD

By Sherman A. Clevenson and Sumner A. Leadbetter

Langley Aeronautical Laboratory
Langley Field, Va.

Washington
December 1956

NATIONAL ADVISORY COMMITTEE FOR AERONAUT

TECHNICAL NOTE 3822

SOME MEASUREMENTS OF AERODYNAMIC FORCES AND MOMENTS AT SUBSONIC SPEEDS ON A WING-TANK CONFIGURATION OSCILLATING IN PITCH ABOUT THE WING MIDCHORD

By Sherman A. Clevenson and Sumner A. Leadbetter

SUMMARY

Measurements are presented of the aerodynamic forces and moments acting on a wing-tank configuration, with or without fins, oscillating in pitch about the wing-root midchord. The reduced-frequency range was from 0.050 to 0.657, whereas the Mach number and Reynolds number ranges were from 0.18 to 0.75 and 0.9×10^6 to 9.5×10^6, respectively.

Comparisons of the experimental aerodynamic forces and moments and their respective phase angles acting on the wing-tank combination with those acting on the wing alone indicated that the overall lifts and moments were greater when the tank was attached. The forces on the tank alone were compared with those determined by an engine-nacelle theory developed by Andropolus, Chee, and Targoff in Air Force Technical Report Number 6353. The agreement between measured and calculated lift was very good.

INTRODUCTION

As a result of the uncertainties and difficulties involved in the analytical treatment of the unsteady aerodynamic forces acting on bodies of revolution such as tip tanks, the validity of flutter analyses for configurations equipped with external stores has been subject to question. Flutter has occurred for wings equipped with tip tanks, and analysis has indicated the possible importance of the air forces contributed by the tanks in influencing the flutter characteristics.

In order to further the knowledge of the unsteady aerodynamic forces on wing-tank configurations, measurements have been made of the air forces acting on a low-aspect-ratio wing equipped with a tip tank oscillating in pitch about the midchord. In order to determine the effect of tank fins, the measurements were made with two different fins and were compared with measurements made with the tank in a clean condition. For comparison, averaged experimental data from a previous investigation for a wing with

an aspect ratio of 2 are shown with the current results of the measurements of the wing—tip-tank combination. The coefficients for the oscillating tank in the presence of an oscillating wing are compared with calculated coefficients for an engine nacelle as determined from a paper by Andropoulos, Chee, and Targoff (ref. 1).

The aerodynamic coefficients are presented for a range of reduced frequency from 0.050 to 0.657 and for a range of Mach numbers from 0.18 to 0.75. The Reynolds number range is from 0.9×10^6 to 9.5×10^6. These measurements were made in the Langley 2- by 4-foot flutter research tunnel by using a resonant-oscillation technique.

SYMBOLS

A	aspect ratio
a	lift-curve slope
a_1	response amplitude to be determined
B,C,R,Y,λ	dummy variables
c	chord of wing, ft
c_r	reference chord
EI	bending stiffness
g	structural damping coefficient
g_t	damping coefficient of wing in airstream
g_{vac}	damping coefficient of wing in a near vacuum
I_e	effective inertia of oscillating system accounting for dynamic deformation of system, ft-lb-sec^2
$i = \sqrt{-1}$	
K	correction
K_s	effective spring constant of oscillating system, ft-lb/radian
k	reduced-frequency parameter, $\omega c/2V$

L oscillating-lift vector acting on the wing for oscillations about the midchord axis, positive when acting upward,

$$L = |L| e^{i(\omega t+\phi_1 \pi/180)} = \pi q S |\alpha| (l_1 + i l_2) e^{i\omega t}$$

$L(x)$ distribution of air load

l_1 nondimensional coefficient of lift in phase with angular displacement

l_2 nondimensional coefficient of lift in phase with angular velocity

$$|l| = \sqrt{l_1^2 + l_2^2}$$

M Mach number

M_α oscillating-moment vector acting on wing for oscillation about midchord, referred to axis of rotation, positive for leading edge up,

$$M_\alpha = |M_\alpha| e^{i(\omega t+\phi_2 \pi/180)} = \pi q S \frac{c}{2} |\alpha| (m_1 + i m_2) e^{i\omega t}$$

m mass of wing

m_r effective reference mass

m_T mass at wing tip

m_1 nondimensional moment coefficient in phase with angular displacement

m_2 nondimensional moment coefficient in phase with angular velocity

P applied aerodynamic loading

p intensity of applied loading

q dynamic pressure, lb/sq ft

S area of wing, sq ft (taken as 1 square foot when used in coefficients)

t time, sec

V velocity of test medium, fps

x	coordinate of wing from root to tip
y	amplitude of wing deflection
y_1	unit tip amplitude
α	angle of attack at midsemispan station as a function of time, $\lvert\alpha\rvert e^{i\omega t}$, radians
γ	root shear
ρ	mass density of test medium, slugs/cu ft
τ	tip of wing
ϕ_1	phase angle that lift vector leads angle of attack, $\tan^{-1}\left(l_2/l_1\right)$, deg
ϕ_2	phase angle that pitching-moment vector leads angle of attack, $\tan^{-1}\left(m_2/m_1\right)$, deg
ϕ_3	phase angle that load leads root shear
ω	circular frequency of oscillation of wing-tank combination, radians/sec
ω_h	circular frequency of first natural wing bending, radians/sec
ω_{vac}	circular frequency of oscillation of wing in a near vacuum, radians/sec

Subscripts:

W	wing in presence of tank
T	tank in presence of wing
WT	wing-tank combination

Dots indicate differentiation with respect to time.

APPARATUS AND METHOD

Tunnel

The Langley 2- by 4-foot flutter research tunnel was used for the present investigation. The test mediums were air or Freon-12 as noted in table I. The use of Freon-12 as a test medium permits the attainment of approximately twice the reduced frequency obtained in air for a given Mach number and frequency.

Model

The model consisted of a 12-inch-span, 12-inch-chord wing with a 5.2-inch-diameter tank, 24 inches long, mounted over the wing tip. (See figs. 1 and 2.) Fabricated construction was employed for the wing; a steel box spar carried four evenly spaced ribs to which plywood skin was attached in order to form an NACA 65A010 airfoil section. The wing was designed to have high natural frequencies in order to reduce the amount of correction to the measured forces due to aeroelastic deformations and to bending inertia loads. (See appendix A.) The first natural cantilever bending frequency of the wing alone was about 130 cycles per second.

The tank was constructed of thin balsa nose and tail sections attached to a thin magnesium center section with ordinates as shown in figure 2. The tank was mounted on a strain-gage balance attached to the wing tip and had a gap with the wing surface of about 1/8 inch. This gap was necessary to isolate the tank from the wing so that only the tank forces and moments would be sensed by the strain-gage balance in the tank. The exposed area of the wing was 0.80 square foot and the plan-form area of the tank was 0.69 square foot.

In order to study the effects of tail fins attached to the tank, some tests were made with the tank equipped with one of two fins. One fin was trapezoidal in shape and the other fin was delta in shape. (See fig. 2.) Both fins had the same area (0.08 square foot) and were mounted so that their centroids of area were the same distance rearward of the pitch axis.

The frequency of the tank on its strain-gage beams was 117 cycles per second, the first bending frequency of the wing-tank combination was 80 cycles per second, and the first torsion of the wing-tank combination was over 150 cycles per second.

The semispan model was mounted as a cantilever beam in an oscillator mechanism at the tunnel wall. This mechanism permitted the model to oscillate in pitch about the midchord axis. The model was mass-balanced about the axis of oscillation in such a way that there were no lift reactions

when the model was oscillated in a near vacuum. During the tests, the frequency of the pitching oscillation of the system varied from 19 to 14 cycles per second.

Oscillator Mechanism

The oscillator mechanism may be considered as a simple, torsional, vibratory system and is illustrated in figure 3. The system consists of a torsion spring which is fixed at one end with the other end attached to a bearing-supported, hollow steel tube to which the model and base plate are clamped. The mechanism was oscillated in torsion at the natural frequency of the simple spring-inertia system by applying a harmonically varying torque through the shaker coils attached to the steel tube. In a near vacuum, this natural frequency was approximately 20 cycles per second.

The bearings were contained in housings which were carried on columns. These columns were designed to include stress-sensitive regions and were equipped with strain gages from which the aerodynamic lift would be determined. The vertical reactions at the fixed end of the torsion spring were negligible because of the flexibility of the torque rod and the small deformations experienced by the strain-gage columns.

The electromagnetic shakers consisted of stationary coils furnishing a steady magnetic field and moving coils which were attached to the steel tube. The moving coils were driven by a variable-frequency oscillator. These moving coils were alined so that the direction of the applied forces was perpendicular to the direction of the lift. Thus, even if a pure torque were not applied to the steel tubes, no resulting force would be sensed by the lift gages. Provision was made for interrupting the power to the moving coils in order to obtain a power-off decaying oscillation.

Instrumentation

The instrumentation was designed to provide continuous signals that were proportional to the lift and angular position and to provide a means of measuring their amplitude and time relationship. The lift reactions were converted to electrical signals by means of wire strain gages attached to the supporting columns. The gages were connected so that only lifting loads were sensed. An electrical signal from a wire strain gage mounted on the torsion spring so as to sense torsional strains was calibrated to give the angular displacement in terms of the wing incidence. The tank was attached at the wing tip through a strain-gage dynamometer so that the tank forces could be separated from the total forces on the combination. The signals were filtered to eliminate noise and higher harmonics, and their magnitudes were measured by using a vacuum-tube voltmeter.

The angular-position signal was recorded on a recording oscillograph during the decay of the oscillation for the purpose of obtaining the damping coefficient.

The phase measurements were made with an electronic counterchronograph. The time lapse between a given point on a lift (or tank moment) signal and a corresponding point on the position signal was measured while the wing-tank combination was oscillated at a constant frequency. The period of oscillation was measured with this instrument by determining the time lapse between corresponding points on the same signal.

Calibration

The angular position of the wing was dynamically calibrated with the signal from the torsion strain gages by a photographic technique. Time exposures were taken of a fine chordwise line on the outer edge of the tank for various amplitudes while the strain-gage output was recorded. The amplitude of oscillation of the wing was obtained from the envelope position of the line on the outer edge of the tank and correlated with the strain-gage signal. By using this procedure and a line on the leading edge of the wing, it was determined that, at the maximum frequency of oscillation (20 cycles per second), the tip angle of incidence exceeded the root angle of incidence by less than 1 percent.

The signals from the balance columns were calibrated in terms of pounds of force per unit of signal strength. Known loads were applied to the wing, and the column reactions were determined by treating the wing shaft system as a simple beam with overhang. (See, for instance, fig. 3.) The reaction forces were then related to the respective signals. The vacuum-tube voltmeter was calibrated dynamically by using a low-frequency oscillator and a voltage divider. These dynamic calibrations were then related to forces by use of the open-circuit load calibration of the strain gages. The readings from the vacuum-tube voltmeter are believed to be within ± 4 percent of true signal.

The phase-measuring system was calibrated at various frequencies by using standard resistance-capacitance phase-shift circuits and by using a cam-operated set of cantilever beams on which strain gages had been mounted. The latter system had distortion and noise and approximated the worst tunnel condition. Calibrations of the phase meter indicated that the phase angle may be determined within $\pm 3^{\circ}$ of true value with a noisy signal and within $\pm 2^{\circ}$ of true value with a clean signal. In order to minimize errors in phase introduced in the electrical operations, a tare value of phase was obtained at each reading by applying either the lift or angular-position signals through both channels of the electrical circuits.

Data Reduction

The total lift forces as received from the balances contain an aerodynamic component and an inertia component which arise from the bending deformation of the wing. In order to correct the measured lift to the aerodynamic lift, it was necessary to correct for the inertia forces due to wing deformation. A discussion of this correction is given in appendix A. The inclusion of this correction leads to a factor which, when multiplied by the measured lift, gives the actual applied lift. The value of this factor is 0.98. In order to estimate possible error incurred by neglecting the aerodynamic forces and moments arising from the bending deformation, these forces were included in the analysis in appendix A and were found to be less than 1 percent of the correction due to wing deformation caused by the inertia forces. The phase angle ϕ_1 contained a component due to these forces that tended to increase ϕ_1 by less than 1°. The moments due to the bending deflection were found to be negligible relative to the magnitude of the measured moment. Since the aerodynamic effects due to wing bending were within the accuracy of the measurement, no effort was made to adjust for these quantities.

The in-phase moment on the wing-tank combination was determined from the change in resonant frequency due to air flowing over the wing and tank as indicated in reference 2. Since the torsional damping was small, its effect on the frequency is neglected and the entire shift is attributed to the in-phase moment. The moment coefficient in phase with the angular displacement is given by

$$m_1 = \frac{-K_s}{\pi q S \frac{c}{2}} \left[\left(\frac{\omega}{\omega_{vac}} \right)^2 - 1 \right]$$

The dependency of m_1 on the small difference of two quantities of approximately the same magnitude leads to considerable loss in accuracy and consequent scatter in the data.

The quadrature-moment coefficient for the wing-tank combination was determined by operating on the time history of the angular position obtained during the power-off decay of the oscillation. The moment coefficient in phase with the angular velocity is given by

$$-m_2 = \frac{I_e \omega^2}{\pi q S \frac{c}{2}} \left[g_t - \left(\frac{\omega_{vac}}{\omega} \right)^2 g_{vac} \right]$$

The derivation of this equation is treated in appendix B.

The phase angle $\phi_{2,WT}$ between the moment vector of the wing-tank combination and the angle of incidence was obtained from the relationship $\phi_{2,WT} = \tan^{-1}(m_2/m_1)_{WT}$. The lack of precision of determining $m_{1,WT}$ and $m_{2,WT}$ directly affects the degree of accuracy of $\phi_{2,WT}$; the values of $\phi_{2,WT}$ are not expected to be more accurate than its components.

The lift forces on the tank were obtained from the outputs of strain-gage balances, and the lift phase angles were determined by using the electronic counterchronograph as discussed in the section entitled "Instrumentation." No correction was made to these lift measurements due to translation of the tank since a calculation of the force due to translation at the worst conditions was less than 1 percent of the measured loads.

The moments on the tank were obtained directly from moment balances and the moment phase angle was determined by using the electronic counterchronograph. However, these measured moments and phase angles were the vector sum of the aerodynamic moments and the inertia moments. The inertia moments were subtracted out vectorially. In some cases, the inertia moments could be large compared with the measured moments. For example, for the condition of $|\alpha| = 0.025$ radian at $M = 0$, the inertia moment was 19 inch-pounds; whereas at $M = 0.75$, the inertia moment was 11 inch-pounds (at a lower frequency) and the measured tank moment was 25 inch-pounds.

The lift, moment, and respective phase angles were determined for the wing in the presence of the tank by a vector subtraction of the tank forces from the forces of the wing-tank combination.

RESULTS

The experimental results for the measured aerodynamic forces, moments, and phase angles for a wing-tank combination and for the tank alone over the end of a low-aspect-ratio wing are given in table I. The forces, moments, and phase angles of the wing in the presence of the attached tank are included. Also, given in this table are the corresponding Mach numbers and reduced frequencies. In order to show trends and comparisons, the experimental values for the wing-tank combination and for the tank alone are also plotted in figures 4 to 11. It may be noted that an investigation to determine the effect of the gap as compared with no gap between the tip tank and the wing indicated that the gap had little effect on the measured forces and phase angles.

DISCUSSION

The total lift and moment coefficients and their respective phase angles for the wing-tank configurations without a fin, with a trapezoidal-shaped fin, and with a delta-shaped fin are discussed first. Further discussion will concern the oscillating lift and moment coefficients and corresponding phase angles for the oscillating tank (oscillating as a unit with the wing in amplitude and frequency).

It should be remembered throughout this discussion that all force and moment coefficients have been obtained by using a reference plan-form area of 1 square foot and a reference chord of one-half wing chord. A constant area was chosen for the presentation of the data in order to facilitate the evaluation of the effects of the tank and fins on the oscillating forces. Thus, for example, any additional lift on the wing-tank combination due to the additional area of the fin should appear as an increase in the coefficient. The actual plan-form areas were as follows: the exposed wing, 0.80 square foot; the tip tank, 0.69 square foot; either the trapezoidal- or delta-shaped fin, 0.08 square foot.

The overall lift coefficients for the various wing-tank combinations are shown in figure 4. Although there is some scatter in the data, the coefficients for the delta fin seem to fall somewhat above the coefficients for the trapezoidal-fin or no-fin condition. For comparison, a solid-line curve representing the average values (from a previous investigation) of experimental lift coefficients for a wing with an aspect ratio of 2 (with no external store) oscillating in pitch about its mid-chord has been shown. Since this solid-line curve appears to be somewhat below the coefficients of the wing-tank combination, it may be deduced that, on a wing with an aspect ratio of 2, the addition of a tip tank, in the manner employed in this investigation, tends to increase the oscillatory lift forces acting on the configuration.

The phase angles for the wing-tank combination corresponding to the overall lift coefficients are shown in figure 5. It may be noted that the phase angles for the three conditions differ only slightly. The phase angles for the condition of no fin on the tank are somewhat greater than for the condition of a fin on the tank. For comparison, the solid-line curve representing average experimental values for a wing alone with an aspect ratio of 2 is shown in this figure. Apparently, there is a small decrease in phase angle on a wing with an aspect ratio of 2 when a tip tank is added, and the addition of a fin on the tank causes a further decrease in the overall lift phase angle.

The total wing-tank oscillating moment coefficients are shown in figure 6 for the three tank-fin configurations. The largest overall moment coefficients are obtained when the tank has no fin on it, and the

lowest coefficients (in these tests) are obtained with the trapezoidal-shaped fin attached in the range of k from 0.1 to 0.5. The moment coefficients obtained when the delta fin is attached are lower than those for the no-fin condition. This decrease in moment coefficient due to the addition of the fin may be caused by the moment contributed by the fin opposing the moment acting on the wing-tank combination. Averaged experimental moment-coefficient data for the wing alone with an aspect ratio of 2 are also shown in figure 6. A comparison of this averaged data with the wing—tip-tank data indicated that the addition of the wing-tip tank (with or without a fin) caused an increase in moment coefficient.

The corresponding phase angles for these wing-tank moment coefficients are shown in figure 7. The data for all three configurations indicate some scatter and there is no pronounced effect of configuration on the moment phase angles. For comparison, a solid-line curve is shown representing average experimental values for a wing alone with an aspect ratio of 2. The moment phase angles are not materially different for the wing alone as compared with the wing with the tip tank.

The forces, moments, and their respective phase angles on the tank while oscillating with the wing were determined for the three fin conditions (no fin, trapezoidal-shaped fin, and delta-shaped fin) and are forthwith discussed. The oscillating-tank lift coefficients are shown in figure 8. The addition of either fin increases the tank lift coefficient as might be expected when it is recalled that the coefficients are reduced by using the same area regardless of plan form. There is little variation of tank lift coefficient as a function of reduced frequency k in the range of k covered. Also shown in figure 8 as a solid-line curve are the results of a theory which was developed for the oscillating air forces on an engine nacelle. This theory (found in appendix IV of ref. 1) accounts only for the nacelle forces acting in front of the quarter chord of the wing and, consequently, gives only a rough representation of the present configuration. A comparison of the experimentally determined oscillating-tank lift coefficients for the configuration of the tank without fins with the results of the nacelle theory indicates very good agreement. A comparison of the magnitude of the oscillating-tank lift coefficients with the steady-state conditions may be made by reference to a recent theoretical paper (ref. 3) which developed the load distributions on wings in steady flow with cylindrical bodies at their tips. An extrapolation of the results of reference 3 indicates that the body at the wing tip contributes about 31 percent of the steady total load on the combination. From a comparison of the oscillating-tank lift coefficients on the tank alone (no fin) in figure 8 with the overall coefficients in figure 4, it is seen that the tank contributes approximately 27 percent of the total load in this oscillating case.

The phase angles by which the tank lift leads the tank position are shown in figure 9. All phase angles increase with increasing k. The addition of either fin caused a decrease in phase angle. A comparison of the phase angles of the tank with overall wing-tank phase angles (fig. 5) indicated the angles to be about the same for the same k. From a comparison of the present experimental data with the theory of reference 1 (nacelle theory), it is seen that the experimental phase angles are higher than the theoretical values for a nacelle for most of the k range covered.

The moment coefficients for the tank by itself (referred to the midchord) are shown in figure 10. The effect of the fin shape (or presence) is indicated, although this effect is not clearly defined because of the scatter in the data. A comparison of the experimental data with the nacelle theory of reference 1 shows that the experimental tank moment coefficients are considerably lower than those predicted by theory for a nacelle.

The tank moment phase angles for the aforementioned moment coefficients are shown in figure 11. The phase angles for all three conditions lie in a scatter band of about 12° with a mean value of -10°. The negative phase angles between moment and position indicate a stabilizing moment. From a comparison of these phase angles with those of the wing-tank combination (fig. 7) it may be seen that the tank phase angles are more or less constant with k, whereas the overall moment phase angles become increasingly negative with k. Also shown in figure 11 are the results of nacelle theory. These phase angles agree fairly well with the measured tank moment phase angles.

CONCLUSIONS

The aerodynamic forces and moments acting on a wing-tank configuration, with or without fins, oscillating in pitch about the wing-root midchord have been measured over the Mach number range from 0.18 to 0.75. Comparisons with similar data obtained in a previous investigation of the same wing without a tip tank indicate the following conclusions:

1. The total lifts and moments of the wing-tank combination were greater than those for the wing alone.

2. The addition of a delta- or trapezoidal-shaped fin on the tip tank caused a decrease in the total moments in contrast to the no-fin condition; however, these moments remained greater than for the wing alone. Furthermore, the moment phase angles were not changed appreciably by the presence of the tank, so that the addition of the tip tank with or without fins had a stabilizing influence on the configuration.

3. The overall lift and moment phase angles did not change greatly with the addition of the tank.

4. The tank lift increased with the addition of either fin.

5. The tank lift and phase angles agreed very well with the results of an engine-nacelle theory, whereas the moment agreement was not so good.

Langley Aeronautical Laboratory,
National Advisory Committee for Aeronautics,
Langley Field, Va., August 2, 1956.

APPENDIX A

CORRECTION OF ROOT REACTION FOR INERTIA AND AEROELASTIC EFFECTS TO DETERMINE THE TOTAL AERODYNAMIC LOAD

In the present experiment on a cantilever wing, knowledge is desired of the total aerodynamic load which develops solely from the torsional oscillations of the wing. This aerodynamic load is not equal precisely to the reaction at the wing root because of the presence of secondary bending reactions which come as a result of the freedom of the wing to be excited slightly in a bending oscillation. A correction must, therefore, be applied to the measured root reaction to obtain the aerodynamic load associated directly with the torsional motion. This appendix derives and shows the magnitude of this correction. The derivation is made in general terms of a wing of variable cross section; the correction is then applied to the uniform wing-tank combination.

On the basis of the engineering beam theory, the differential equation for bending of the wing is

$$(1 + ig)\frac{\partial^2}{\partial x^2} EI \frac{\partial^2 y}{\partial x^2} = p \tag{A1}$$

where g is the structural damping coefficient and p is the intensity of the applied loading. With the choice of a strip-analysis approach, the loading for the case under consideration may be written

$$p = -m\ddot{y} - \frac{\pi\rho c^2}{4}\ddot{y} - \frac{a}{2}\rho cV(F + iG)\dot{y} + P \tag{A2}$$

The first term in this expression is the inertia force associated with the wing mass; the second and third terms refer, respectively, to the apparent air-mass inertia effect and the aerodynamic damping associated with bending oscillations; and the fourth term refers to the torsionally induced aerodynamic loading, which herein is regarded as the applied forcing function. The second and third terms were established by using oscillating-flow theory for two-dimensional incompressible flow as a guide; the lift-curve slope a and the F and G coefficients, which are like the in-phase and out-of-phase Theodorsen flutter coefficients, are to be selected as appropriate to the case being treated.

Since harmonic motion is involved, the loading and the deflection may be written, respectively,

$$P = L(x)e^{i\omega t} \tag{A3a}$$

$$y = Y(x)e^{i\omega t} \tag{A3b}$$

Now, with the use of equations (A2) and (A3), equation (A1) reduces to

$$(1 + ig)\frac{d^2}{dx^2} EI \frac{d^2y}{dx^2} = \omega^2 \overline{m} Y - i \frac{a}{2} \rho c V \omega (F + iG)Y + L \tag{A4}$$

where

$$\overline{m} = m + \frac{\pi \rho c^2}{4}$$

A convenient and fairly accurate approximate solution to this equation can be obtained by expressing the deflection in terms of the fundamental bending vibration mode of the wing; the choice here of only a single-mode expansion is considered adequate since the forcing frequencies used in the experiments were below the fundamental wing frequency. Thus,

$$Y = a_1 y_1 \tag{A5}$$

where a_1 represents the response amplitude to be determined and y_1 is given in terms of unit tip amplitude and satisfies the equation

$$\frac{d^2}{dx^2} EI \frac{d^2 y_1}{dx^2} = \omega_n^2 \overline{m} y_1 \tag{A6}$$

In accordance with the Galerkin procedure for solving differential equations, equation (A5) is substituted into equation (A4) which is then multiplied by y_1 and integrated over the length of the wing. The result, with the use of equation (A6), is

$$a_1(1 + ig)\omega_n^2 J = a_1 \omega^2 J - i a_1 \frac{a}{\pi} \frac{m_r}{k} \omega^2 (F + iG)H + \int_0^\tau L y_1 \, dx \tag{A7}$$

where

$$J = \int_0^T \overline{m} y_1^2 dx + m_T$$

$$H = \int_0^T \frac{c}{c_r} y_1^2 dx$$

$$m_r = \frac{\pi \rho c_r^2}{4}$$

$$k = \frac{\omega c_r}{2V}$$

m_T is the mass at the wing tip, and c_r is some convenient reference chord which is usually taken at approximately the three-quarter-span station. The desired response amplitude can now be determined directly from equation (A7); hence,

$$a_1 = \frac{\int_0^T L y_1 \, dx}{\left(\omega_h^2 - \omega^2\right) J - \frac{a}{\pi} \frac{G}{k} m_r H \omega^2 + i \left(g \omega_h^2 J + \frac{a}{\pi} \frac{F}{k} m_r H \omega^2 \right)} \tag{A8}$$

The loading on the beam is now written in terms of a_1. Substitution of equations (A3) and (A5) into equation (A2) gives

$$p = \left\{ \left[m \omega_h^2 y_1 + \frac{\pi \rho c^2}{4} \omega^2 y_1 - i \frac{a}{2} \rho c V \omega (F + iG) y_1 \right] a_1 + L \right\} e^{i\omega t}$$

The root shear or reaction, which may be designated $\gamma e^{i\omega t}$, may be found by integrating this loading over the length of the beam; thus,

$$\gamma e^{i\omega t} = \left\{ \left[\omega^2 N_1 - i(F + iG) \frac{a}{\pi} \frac{m_r \omega^2}{k} B_1 \right] a_1 + \int_0^T L \, dx \right\} e^{i\omega t} \tag{A9}$$

where

$$N_1 = \int_0^\tau \bar{m} y_1 \, dx + m_\tau$$

$$B_1 = \int_0^\tau \frac{c}{c_r} y_1 \, dx$$

Substitution of equation (A8) into equation (A9) and cancellation of the harmonic terms gives

$$\gamma = \left[1 + \frac{(C_1 + iC_2)d}{D_1 + iD_2} \right] \int_0^\tau L \, dx \tag{A10}$$

where

$$\left.\begin{aligned} C_1 &= \frac{N_1}{J} + \frac{a}{\pi} \frac{G}{k} \frac{m_r B_1}{J} \\ C_2 &= -\frac{a}{\pi} \frac{F}{k} \frac{m_r B_1}{J} \\ D_1 &= \frac{\omega_h^2}{\omega^2} - 1 - \frac{a}{\pi} \frac{G}{k} \frac{m_r H}{J} \\ D_2 &= g \frac{\omega_h^2}{\omega^2} + \frac{a}{\pi} \frac{F}{k} \frac{m_r H}{J} \\ d &= \frac{\int_0^\tau L y_1 \, dx}{\int_0^\tau L \, dx} \end{aligned}\right\} \tag{A11}$$

As stated earlier, knowledge is desired of the total aerodynamic load that is associated with the torsional oscillations of the wing. This total load is found directly from equation (A10) to be

$$\int_0^\tau L \, dx = \frac{D_1 + iD_2}{C_1 d + D_1 + i(C_2 d + D_2)} \gamma$$

This equation, when expressed in the complex notation of a modulus and phase angle, becomes

$$\int_0^\tau L\,dx = \sqrt{\frac{D_1^2 + D_2^2}{(C_1 d + D_1)^2 + (C_2 d + D_2)^2}}\, e^{i\phi_3}\gamma = Ke^{i\phi_3}\gamma \qquad (A12)$$

where

$$\phi_3 = \tan^{-1}\frac{(C_1D_2 - C_2D_1)d}{d(C_1D_1 + C_2D_2) + D_1^2 + D_2^2} \qquad (A13)$$

Equation (A13) is the final equation sought. Thus, the magnitude of the torsionally induced air load is found simply by multiplying the correction K by the magnitude of the measured root shear; the phase angle between this load and the root shear is given by ϕ_3. A word about the coefficients C_n, D_n, and d may now be in order. All terms in these coefficients which contain the lift-curve slope a are related to the aerodynamic damping effects associated with the bending oscillations. A comparison of the second term with the first term in D_2, for example, will indicate how strong the aerodynamic damping is in relation to the structural damping. The nondimensional term d may be seen to depend on the distribution of the air load L(x). For most practical cases, it is considered sufficient to evaluate this factor on the basis that the air load has an elliptic distribution.

Some simplification results when the aforementioned relations are applied to the case treated herein, that is, to a uniform cantilever wing with a mass at its tip. When the assumption is made that there is no change in mode shape of a cantilever wing due to the mass at its tip, it can be shown that

$$\left.\begin{aligned} J &= \bar{m}\int_0^\tau y_1^2 dx + m_\tau = \frac{\bar{m}\tau}{4} + m_\tau \\ N_1 &= \bar{m}\int_0^\tau y_1\,dx + m_\tau = 0.39\,\bar{m}\tau + m_\tau \\ H &= \int_0^\tau y_1^2 dx = \frac{\tau}{4} \\ B_1 &= \int y_1\,dx = 0.39\tau \end{aligned}\right\} \qquad (A14)$$

Hence,

$$\left.\begin{aligned} C_1 &= \frac{0.39\,\overline{m}_T + m_T}{\frac{\overline{m}_T}{4} + m_T} + \frac{a}{\pi}\frac{G}{k}\frac{m_r(0.39\tau)}{m_T + \frac{\overline{m}_T}{4}} \\ C_2 &= -\frac{a}{\pi}\frac{F}{k}\frac{m_r(0.39\tau)}{\frac{\overline{m}_T}{4} + m_T} \\ D_1 &= \frac{\omega_n^2}{\omega^2} - 1 - \frac{a}{\pi}\frac{G}{k}\frac{m_r\frac{\tau}{4}}{\frac{\overline{m}_T}{4} + m_T} \\ D_2 &= g\frac{\omega_n^2}{\omega^2} + \frac{a}{\pi}\frac{F}{k}\frac{m_r\frac{\tau}{4}}{\frac{\overline{m}_T}{4} + m_T} \end{aligned}\right\} \qquad \text{(A15a)}$$

and, for an assumed elliptic loading,

$$d = 0.29 \qquad \text{(A15b)}$$

In order to determine the correction K and the phase angle ϕ_3, equations (A12) and (A13) were used together with equations (A15). The structural damping coefficient used for the wing was $g = 0.008$. The lift-curve slope was taken equal to the theoretical value of 2π multiplied by the often-used aspect-ratio correction $\frac{A}{A + 2}$, and was thus taken as π since the wing has an aspect ratio of 2. The F and G functions were arbitrarily chosen as those for two-dimensional incompressible flow.

In order to gain an insight as to how aerodynamic-damping effects compare with structural-damping effects, the calculations were made for two conditions: (1) with structural damping only and (2) with both structural and aerodynamic damping included. No differences are noted in K for these two conditions. The following table shows the results for these two conditions for a frequency of 20 cycles per second:

Structural damping only, a = 0		Both structural and aerodynamic damping	
K	ϕ_3, deg	K	ϕ_3, deg
0.98	0.01	0.98	0.05

Although a difference in phase angle is noted for the two damping conditions, the important item to note is that in both cases the phase angle is a negligible quantity.

APPENDIX B

DETERMINATION OF THE AERODYNAMIC DAMPING-MOMENT COEFFICIENT

In this appendix the method used in obtaining the aerodynamic damping-moment coefficient from the power-off decaying oscillations of a torsional spring-inertia system is given. By assuming a linear system, particularly with respect to the aerodynamic coefficients, and by using the concept that the structural damping moment is in phase with the angular velocity but proportional to the angular displacement, the differential equation of motion of the system may be given by

$$I_e\ddot{\alpha} + K_s\left(1 + ig_{vac}\right)\alpha = \pi qS\,\frac{c}{2}\,\alpha\left(m_1 + im_2\right) \tag{B1}$$

or

$$\ddot{\alpha} + \frac{C + iB}{R}\,\alpha = 0$$

By definition,

$$\frac{C}{R} = \frac{K_s - \pi qS\,\frac{c}{2}\,m_1}{I_e} = \omega^2$$

and

$$\frac{B}{C} = \frac{K_s g_{vac} - \pi qS\,\frac{c}{2}\,m_2}{K_s - \pi qS\,\frac{c}{2}\,m_1} = \lambda$$

Equation (B1) has a solution of the following form (see, for instance, page 86 of ref. 4):

$$\alpha = |\alpha|\,e^{\sqrt{\frac{C}{2R}}\left[-\sqrt{\left(1+\lambda^2\right)^{1/2}-1}+\sqrt{i\left(1+\lambda^2\right)^{1/2}+1}\right]t} \tag{B2}$$

For small values of λ, equation (B2) becomes

$$\alpha = |\alpha|\,e^{\omega t\left[-\frac{\lambda}{2}+i\left(1+\frac{\lambda^2}{4}\right)\right]} \approx |\alpha|\,e^{\omega t\left(-\frac{\lambda}{2}+i\right)} \tag{B3}$$

For the logarithmic decrement, equation (B3) at $t = 0$ becomes

$$|\alpha|_0 = |\alpha|$$

and, after n cycles, at $t = 2\pi n/\omega$,

$$|\alpha|_n = |\alpha| e^{-\pi\lambda n}$$

or

$$\frac{|\alpha|_0}{|\alpha|_n} = e^{\pi\lambda n} \tag{B4}$$

By taking the natural logarithm of both sides of equation (B4),

$$\lambda = \frac{1}{\pi n} \log_e \frac{|\alpha|_0}{|\alpha|_n} = g_t$$

which is measured with the wing subjected to air flow. In the equation for λ,

$$g_t = \frac{K_s g_{vac} - \pi q S \frac{c}{2} m_2}{K_s - \pi q S \frac{c}{2} m_1} \tag{B5}$$

Since

$$K_s - \pi q S \frac{c}{2} m_1 = I_e \omega^2$$

and

$$K_s = I_e \omega_{vac}^2$$

then

$$-m_2 = \frac{I_e \omega^2}{\pi q S \frac{c}{2}} \left[g_t - \left(\frac{\omega_{vac}}{\omega} \right)^2 g_{vac} \right] \tag{B6}$$

Equation (B6) is the form used in the reduction of the damping-moment data in this paper.

REFERENCES

1. Andropoulos, T. C., Chee, C. F., Targoff, W. P.: The Effect of Engine Locations on the Antisymmetric Flutter Mode. AF Tech. Rep. No. 6353, Air Research and Development Command, U. S. Air Force, Aug. 1951.

2. Clevenson, Sherman A., and Widmayer, Edward, Jr.: Experimental Measurements of Forces and Moments on a Two-Dimensional Oscillating Wing at Subsonic Speeds. NACA TN 3686, 1956. (Supersedes NACA RM L9K28a.)

3. Hartley, D. E.: Theoretical Load Distributions on Wings With Cylindrical Bodies at the Tips. C.P. No. 147, British A.R.C., 1954.

4. Scanlan, Robert H., and Rosenbaum, Robert: Introduction to the Study of Aircraft Vibration and Flutter. The MacMillian Co., 1951.

TABLE I.- RESULTS OF AN EXPERIMENTAL INVESTIGATION ON A WING-TANK CONFIGURATION

(a) No fin on the tank

k	M	$\lvert z\rvert_{WT}$	$\phi_{1,WT}$	$\lvert z\rvert_{T}$	$\phi_{1,T}$	$\lvert z\rvert_{W}$	$\phi_{1,W}$	$\lvert M\alpha\rvert_{WT}$	$\phi_{2,WT}$	$\lvert M\alpha\rvert_{T}$	$\phi_{2,T}$	$\lvert M\alpha\rvert_{W}$	$\phi_{2,W}$	Medium
0.050	0.69	1.03	-5	0.28	-3	0.75	-8	0.72	-3	0.25	-7	0.47	-1	
.053	.67	1.08	-5	.29	-2	.79	-8	.74	-3	.24	-7	.50	-1	
.093	.50	1.02	-2	.26	3	.76	-2	.69	-6	.18	-10	.51	-5	Air
.099	.48	1.12	-2	.28	3	.84	-2	.68	-6	.19	-10	.49	-4	
.109	.45	1.05	0	.27	5	.78	0	.66	-6	.17	-12	.49	-4	
.117	.42	1.14	1	.28	6	.86	-1	.66	-7	.18	-13	.48	-5	
.127	.60	1.17	-2	.25	2	.92	-3	.64	-----	.27	-7	-----	----	Freon-12
.128	.40	1.07	2	.26	8	.81	1	.63	-8	.14	-10	.49	-7	Air
.143	.58	1.03	0	.23	2	.80	-1	.62	-----	.22	-5	-----	----	Freon-12
.151	.55	1.18	3	.25	6	.93	2	.66	-----	.28	-7	-----	----	
.159	.33	.98	4	.25	12	.64	1	.60	-15	.08	-14	.47	-15	Air
.168	.52	1.07	2	.23	8	.84	1	.69	-8	.25	-8	.44	-8	
.182	.51	1.06	3	.23	5	.83	2	.67	-12	.24	-8	.43	-14	
.191	.48	1.07	8	.24	9	.83	8	.68	-10	.25	-8	.43	-11	
.207	.46	1.07	6	.24	10	.83	5	.70	-11	.24	-8	.46	-12	
.228	.44	1.06	8	.23	12	.83	7	.67	-11	.24	-8	.43	-13	
.254	.41	1.10	8	.24	12	.86	7	.65	-16	.24	-8	.41	-21	
.275	.38	1.06	12	.23	15	.83	11	.65	-17	.22	-9	.43	-21	
.316	.34	1.03	13	.24	16	.79	12	.73	-12	.21	-8	.52	-14	Freon-12
.319	.34	1.03	15	.25	19	.78	14	.72	-17	.22	-8	.50	-21	
.399	.28	1.03	21	.25	24	.78	20	.84	-24	.20	-8	.65	-29	
.458	.26	1.08	23	.25	27	.83	22	-----	-41	.15	-8	-----	----	
.492	.23	1.09	25	.28	29	.81	24	.84	-38	.19	-8	.68	-46	
.555	.21	1.11	30	.30	31	.81	30	.98	-30	.16	-6	.84	-34	
.638	.18	1.20	32	.34	33	.86	31	1.18	-36	.15	-7	1.05	-40	

TABLE I.- RESULTS OF AN EXPERIMENTAL INVESTIGATION ON A WING-TANK CONFIGURATION - Continued

(b) Trapezoidal-shaped fin on the tank

k	M	$\lvert z \rvert_{WT}$	$\phi_{1,WT}$	$\lvert z \rvert_{T}$	$\phi_{1,T}$	$\lvert z \rvert_{W}$	$\phi_{1,W}$	$\lvert M_\alpha \rvert_{WT}$	$\phi_{2,WT}$	$\lvert M_\alpha \rvert_{T}$	$\phi_{2,T}$	$\lvert M_\alpha \rvert_{W}$	$\phi_{2,W}$	Medium
0.066	0.65	1.06	-3	0.38	-4	0.68	-2	0.60	-5	0.13	-5	0.47	-5	
.074	.62	1.07	-3	.40	-2	.67	-4	.58	-4	.13	-6	.45	-3	
.084	.56	1.14	-3	.40	-2	.74	-4	.57	-6	.13	-7	.44	-6	Air
.096	.51	1.09	-1	.40	-1	.69	-1	.52	-6	.10	-6	.42	-6	
.122	.42	1.02	-1	.37	-1	.65	-1	.48	-8	.06	-12	.42	-7	
.129	.62	1.19	-3	.40	-4	.79	-2	.60	-----	.15	-9	-----	----	
.156	.59	1.19	0	.38	-5	.81	2	.50	-17	.15	-9	.35	-20	
.167	.55	1.20	-1	.37	-3	.83	-1	.54	-16	.12	-7	.42	-19	
.185	.52	1.16	1	.36	-1	.80	1	.55	-12	.20	-11	.35	-13	
.201	.49	1.18	5	.38	0	.80	7	.47	-21	.27	-15	.20	-29	
.223	.47	1.12	1	.35	0	.77	1	.54	-13	.19	-11	.35	-14	
.242	.43	1.13	5	.33	2	.80	6	.55	-17	.18	-10	.37	-20	Freon-12
.263	.41	1.13	5	.35	3	.78	6	.52	-17	.25	-14	.27	-20	
.293	.37	1.11	9	.38	7	.73	10	.53	-21	.18	-10	.35	-27	
.310	.34	1.09	10	.36	10	.73	10	.55	-25	.28	-16	.28	-34	
.316	.35	1.03	12	.29	12	.74	12	.62	-17	.31	-17	.31	-17	
.371	.30	1.08	14	.37	14	.71	14	.57	-27	.30	-17	.28	-38	
.414	.27	1.04	17	.32	17	.72	17	.49	-38	.25	-14	.28	-59	
.499	.23	1.04	24	.35	23	.69	25	.56	-55	.21	-11	.43	-75	

TABLE I.- RESULTS OF AN EXPERIMENTAL INVESTIGATION ON A

WING-TANK CONFIGURATION - Concluded

(c) Delta-shaped fin on the tank

k	M	$\lvert z\rvert_{WT}$	$\phi_{1,WT}$	$\lvert z\rvert_{T}$	$\phi_{1,T}$	$\lvert z\rvert_{W}$	$\phi_{1,W}$	$\lvert M\alpha\rvert_{WT}$	$\phi_{2,WT}$	$\lvert M\alpha\rvert_{T}$	$\phi_{2,T}$	$\lvert M\alpha\rvert_{W}$	$\phi_{2,W}$	Medium
0.051	0.75	1.00	-5	0.42	-4	0.58	-6	0.62	-7	0.08	-7	0.54	-7	
.060	.70	.99	-4	.42	-4	.57	-4	.56	-6	.08	-9	.48	-6	
.069	.63	.93	-3	.42	-3	.51	-3	.59	-5	.06	-8	.53	-5	Air
.076	.58	1.07	-4	.43	-4	.64	-4	.55	-8	.05	-16	.50	-7	
.079	.57	.99	-3	.45	-3	.54	-3	.52	-9	.052	-11	.47	-9	
.087	.55	1.04	-3	.42	-2	.47	-4	.49	-6	.054	-17	.47	-5	
.134	.62	1.22	-4	.40	-2	.82	-5	.54	-----	.09	-5	-----	----	
.146	.59	1.20	-2	.38	-1	.82	-2	.55	-----	.14	-8	-----	----	
.156	.57	1.28	-1	.37	0	.91	-1	.56	-8	.10	-6	.46	-8	
.168	.54	1.24	-2	.39	1	.85	-3	.57	-10	.12	-7	.45	-11	
.179	.52	1.25	0	.34	1	.91	1	.61	-11	.16	-9	.45	-12	
.189	.51	1.26	1	.32	2	.94	1	.62	-15	.16	-9	.46	-17	
.195	.49	1.19	0	.34	2	.85	-1	.60	-12	.14	-8	.46	-13	
.212	.46	1.21	2	.32	3	.89	2	.62	-12	.15	-9	.47	-13	
.233	.43	1.20	3	.34	5	.86	2	.64	-12	.16	-9	.48	-13	
.261	.40	1.23	4	.34	5	.89	4	.62	-14	.18	-10	.44	-16	Freon-12
.288	.37	1.17	7	.33	8	.84	7	.60	-18	.17	-9	.43	-22	
.320	.34	1.16	10	.31	11	.85	10	.70	-19	.13	-7	.57	-22	
.324	.34	1.12	10	.33	12	.79	9	.62	-25	.17	-10	.46	-31	
.374	.29	1.17	13	.31	15	.86	12	.77	-22	.16	-9	.62	-25	
.420	.27	1.15	16	.32	18	.83	15	.78	-27	.12	-7	.67	-31	
.492	.24	1.18	23	.33	23	.85	23	.71	-33	.15	-8	.58	-39	
.560	.21	1.17	25	.36	27	.81	24	.88	-33	.25	-14	.65	-40	
.657	.18	1.18	34	.39	34	.79	34	.97	-49	.31	-17	.73	-62	

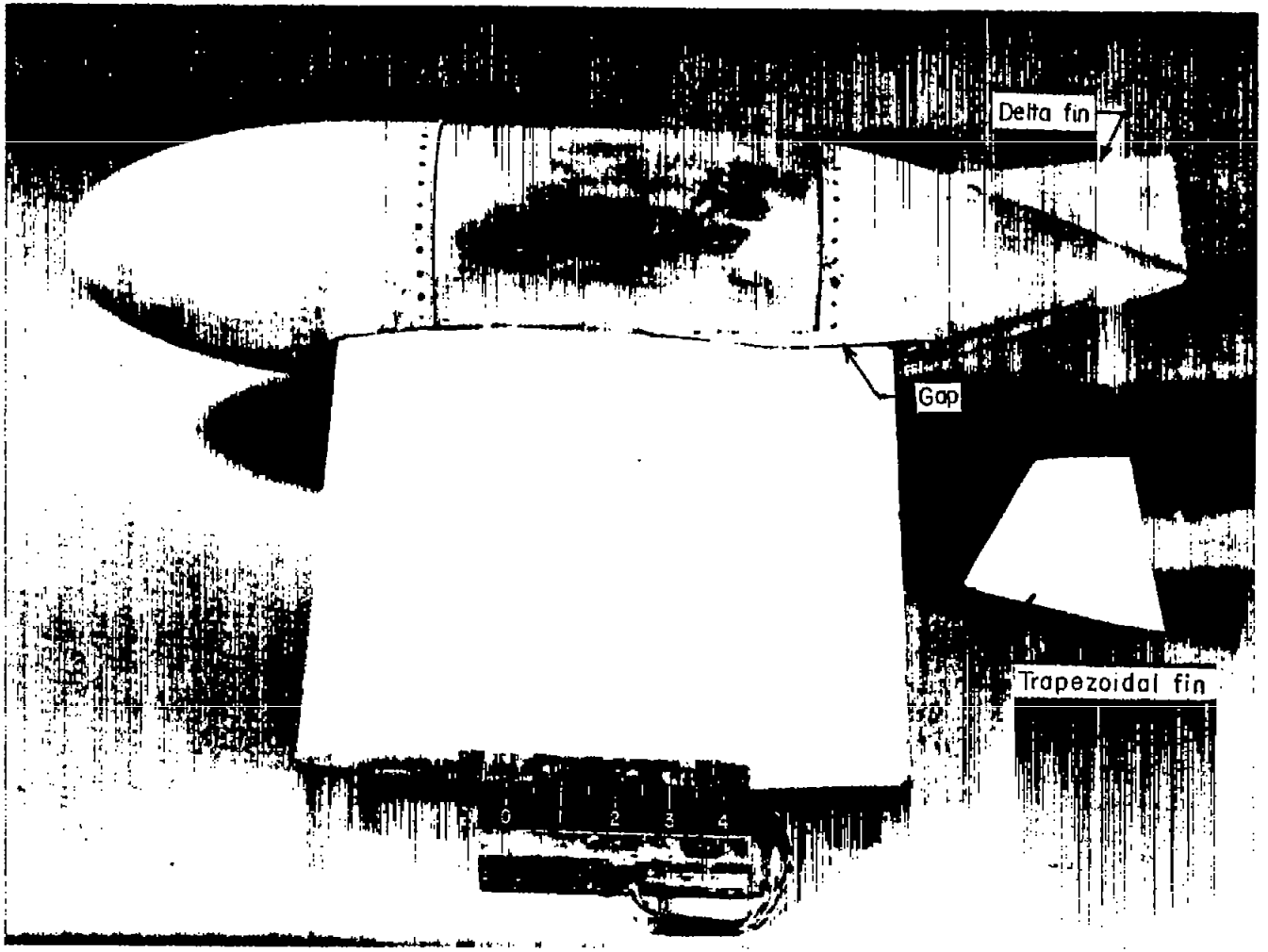

L-86047.2

Figure 1.- Photograph of wing-tank combination.

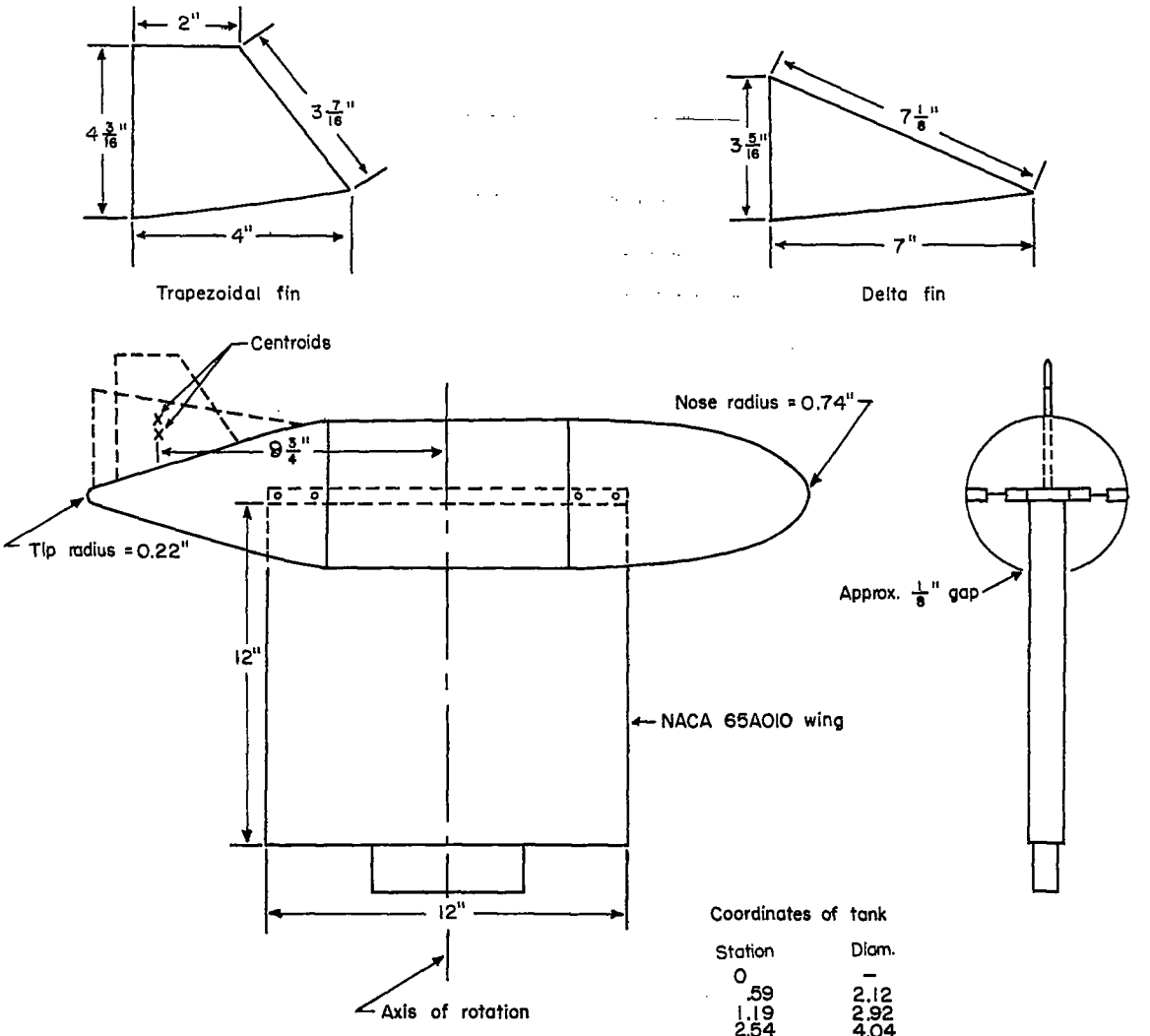

Figure 2.- Diagrammatic view showing various fins of wing-tank combination.

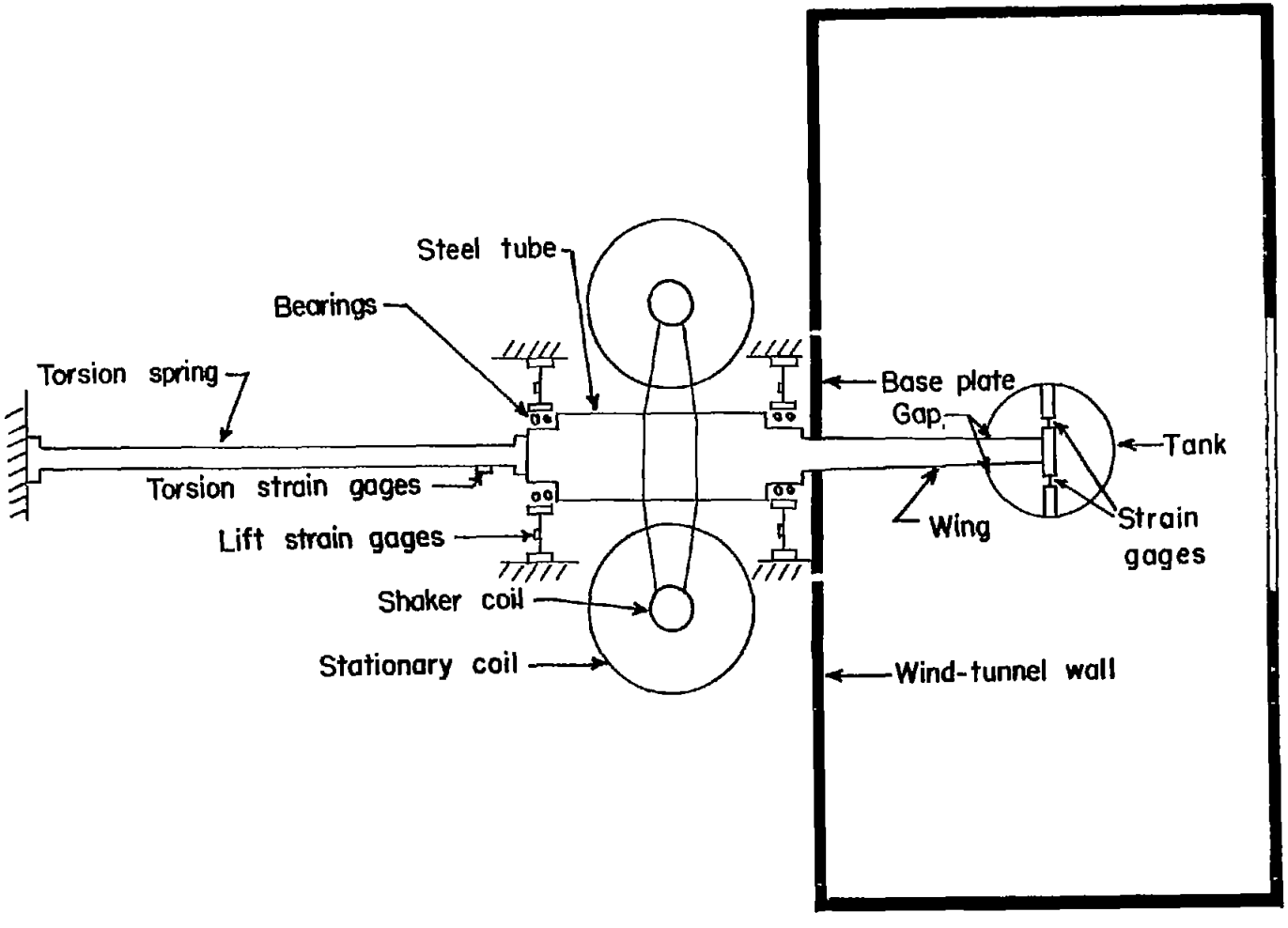

Figure 3.- Diagrammatic view of oscillator mechanism and wing-tank combination mounted in the Langley 2- by 4-foot flutter research tunnel.

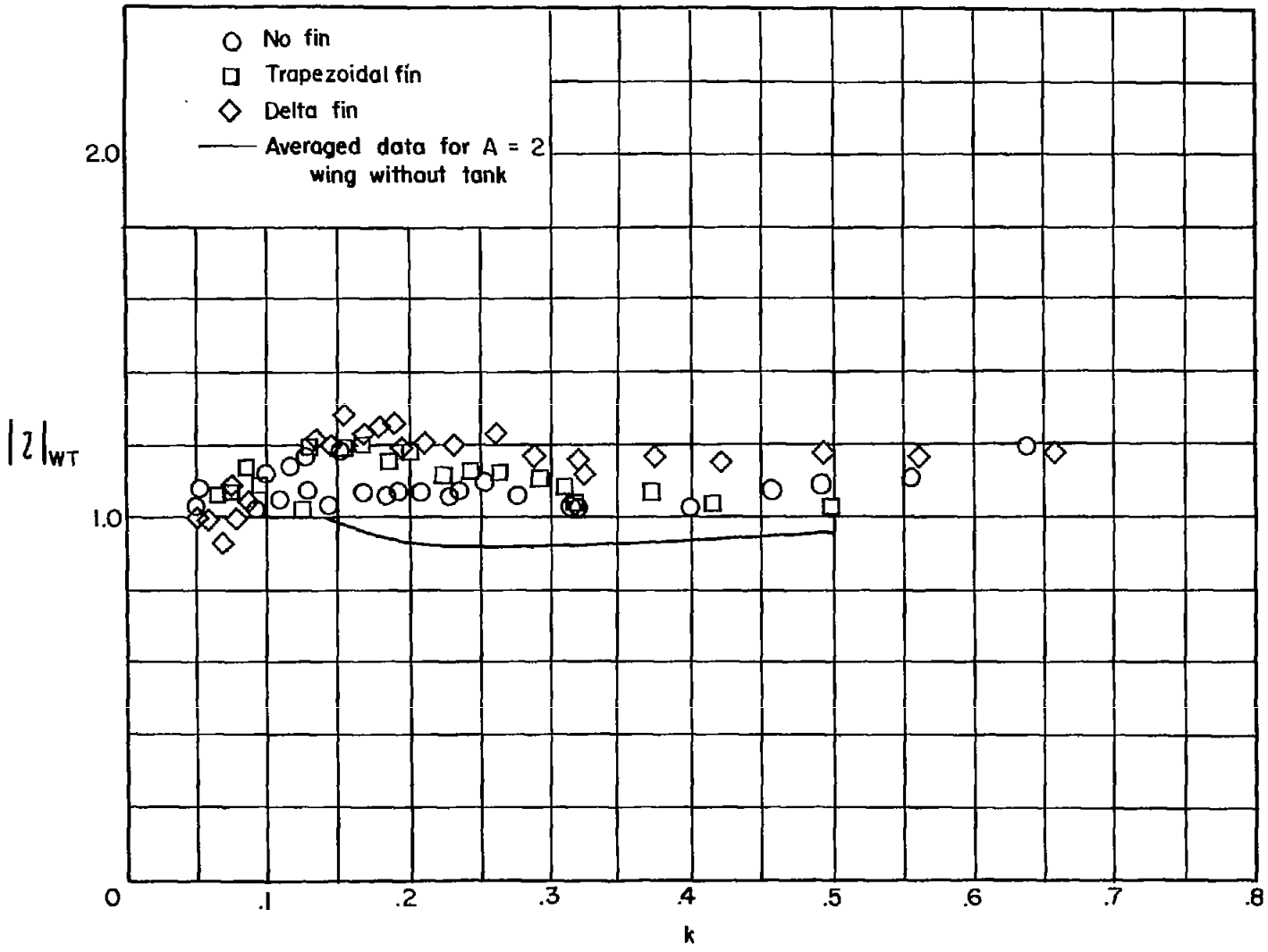

Figure 4.- Variation of total experimental lift coefficients with reduced frequency for the oscillating wing-tank combination.

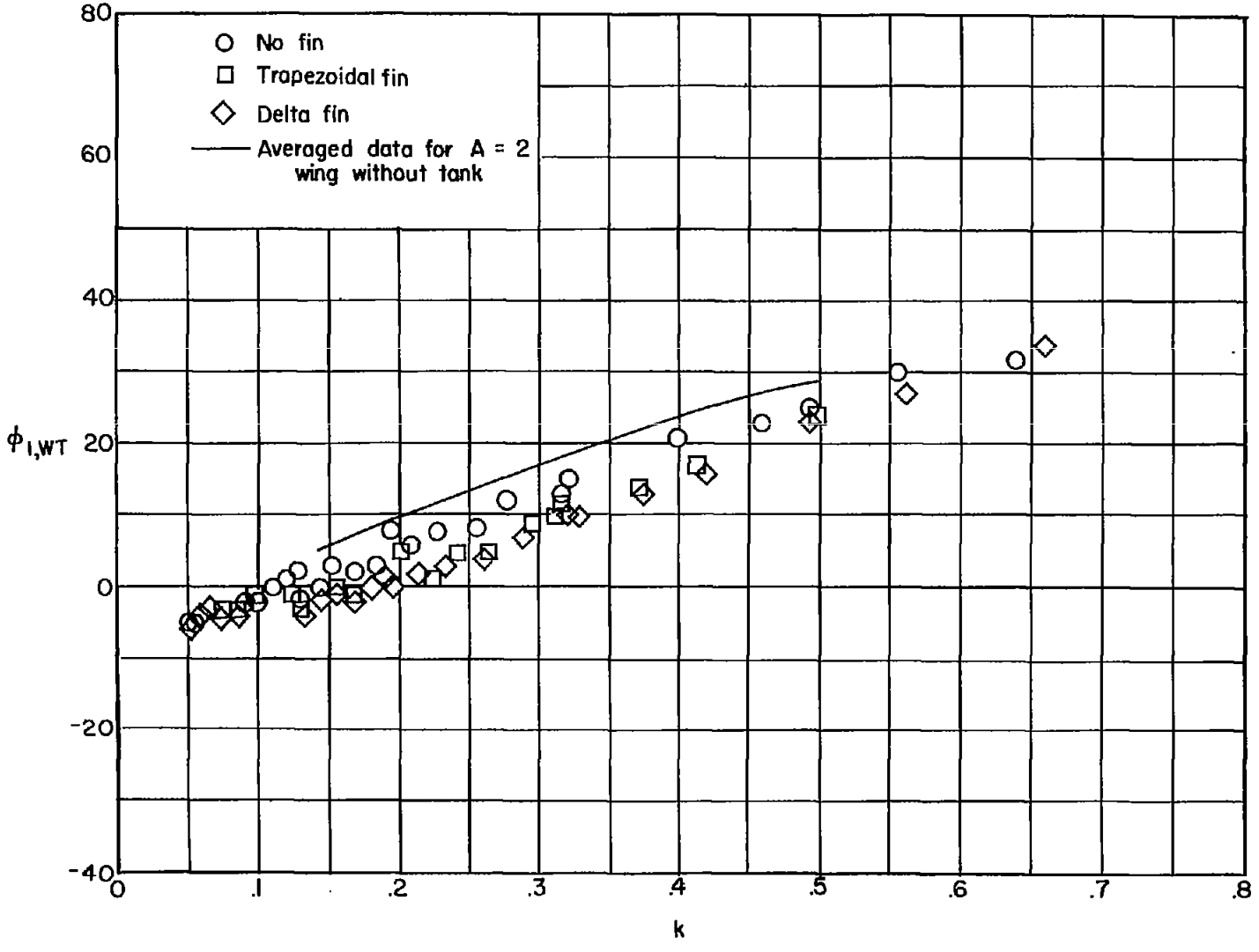

Figure 5.- Variation of total experimental lift phase angles with reduced frequency for the oscillating wing-tank combination.

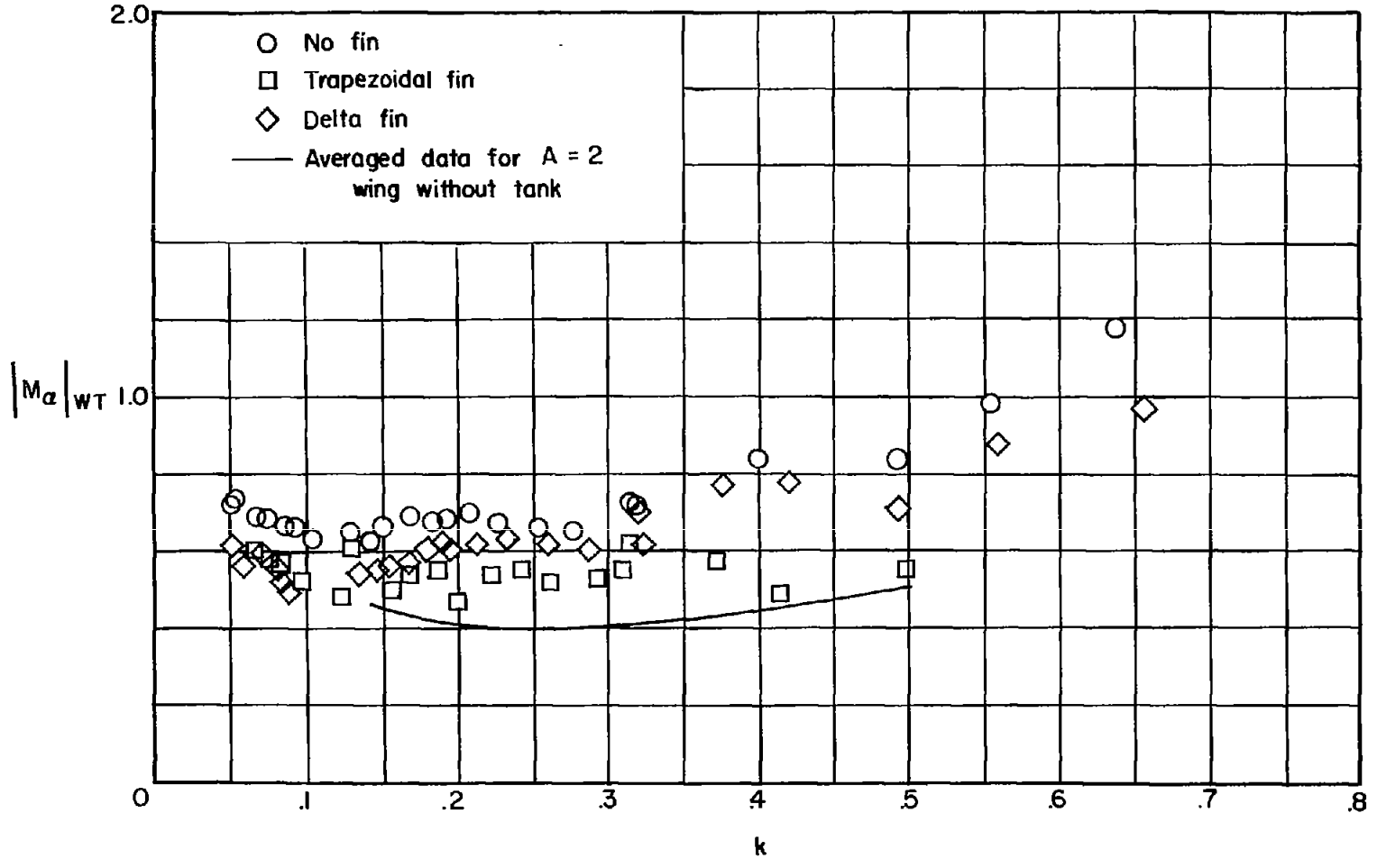

Figure 6.- Variation of total experimental moment coefficients with reduced frequency for the oscillating wing-tank combination.

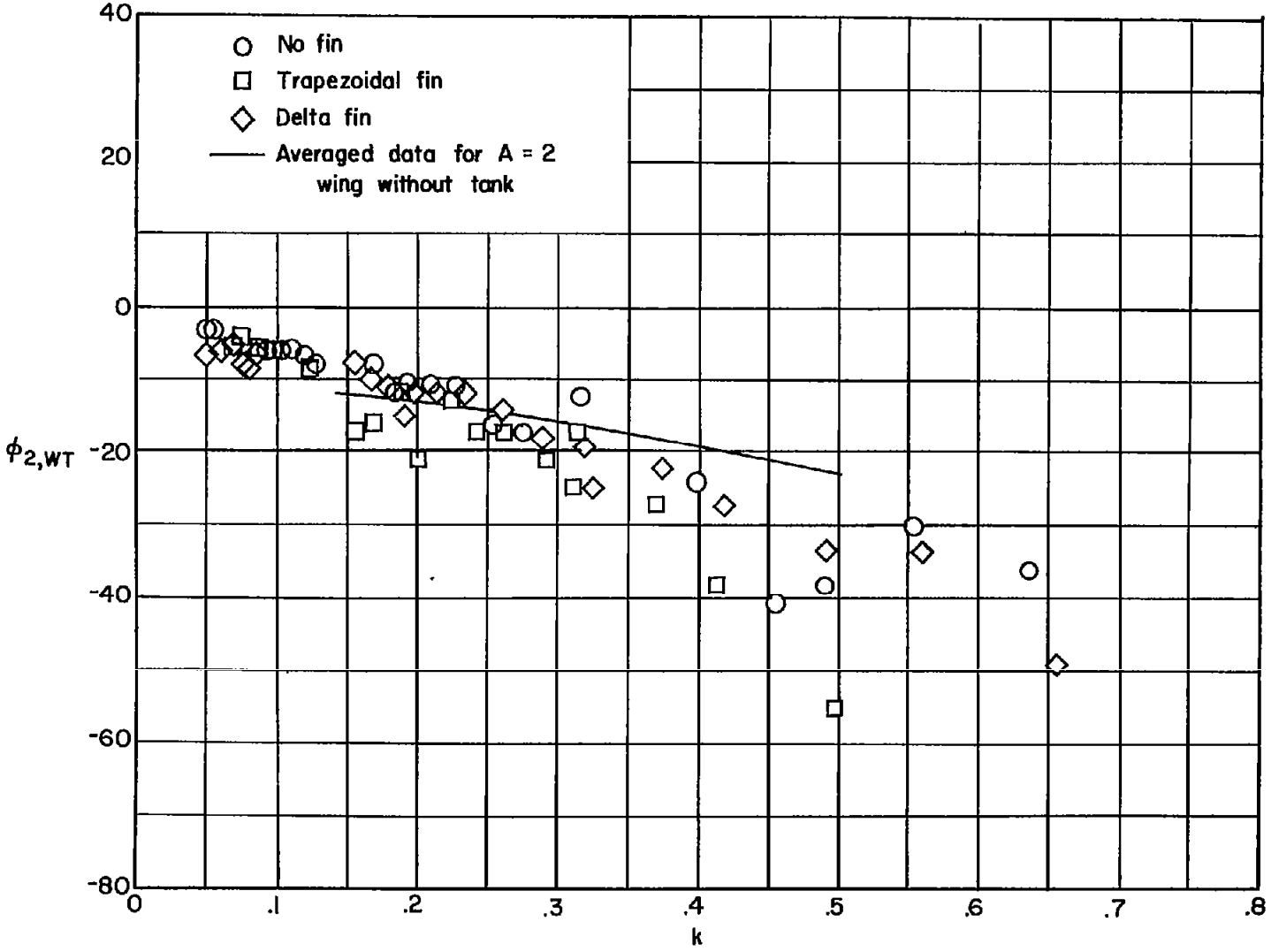

Figure 7.- Variation of total experimental moment phase angles with reduced frequency for the oscillating wing-tank combination.

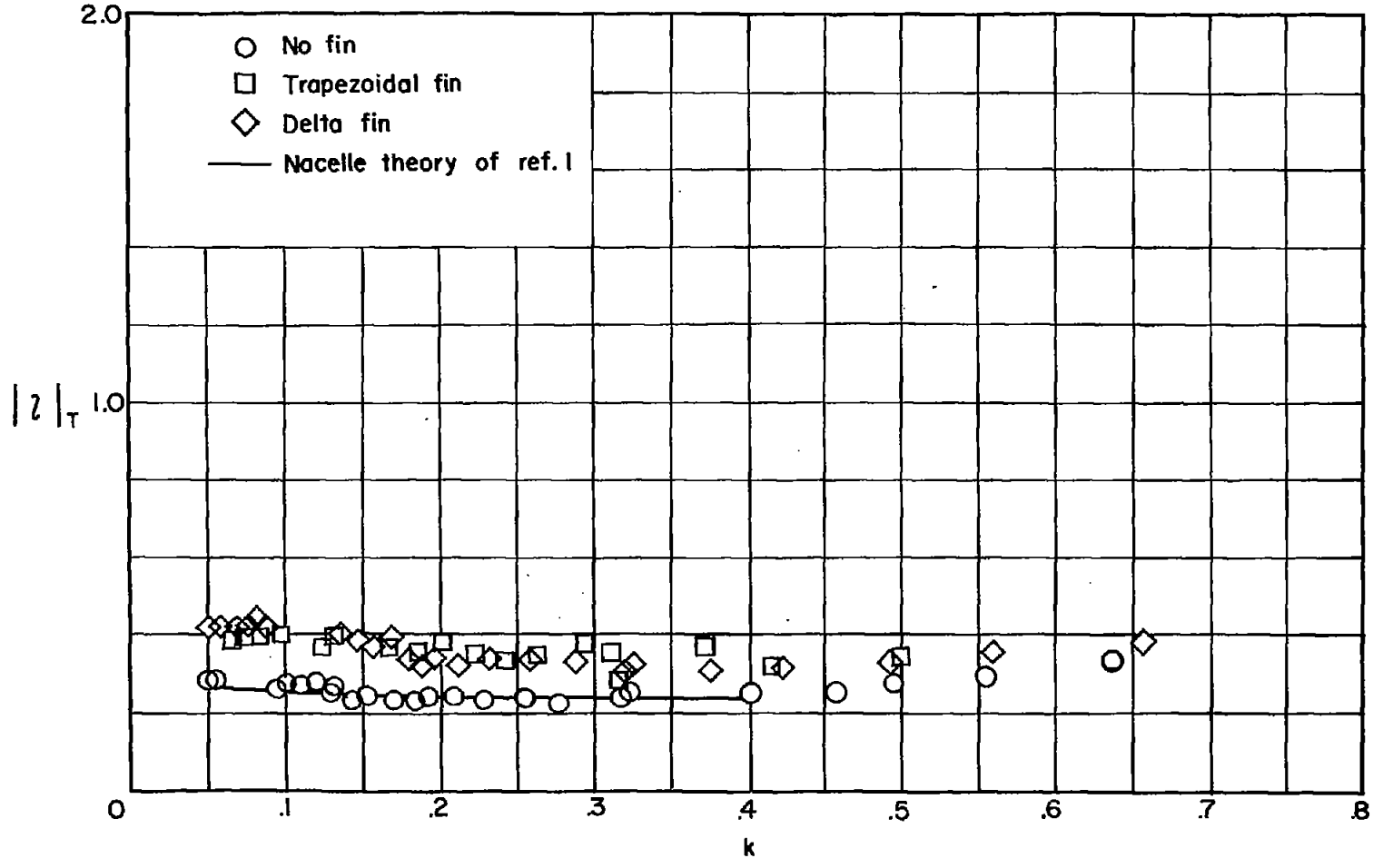

Figure 8.- Variation of experimental lift coefficient with reduced frequency for the oscillating tank.

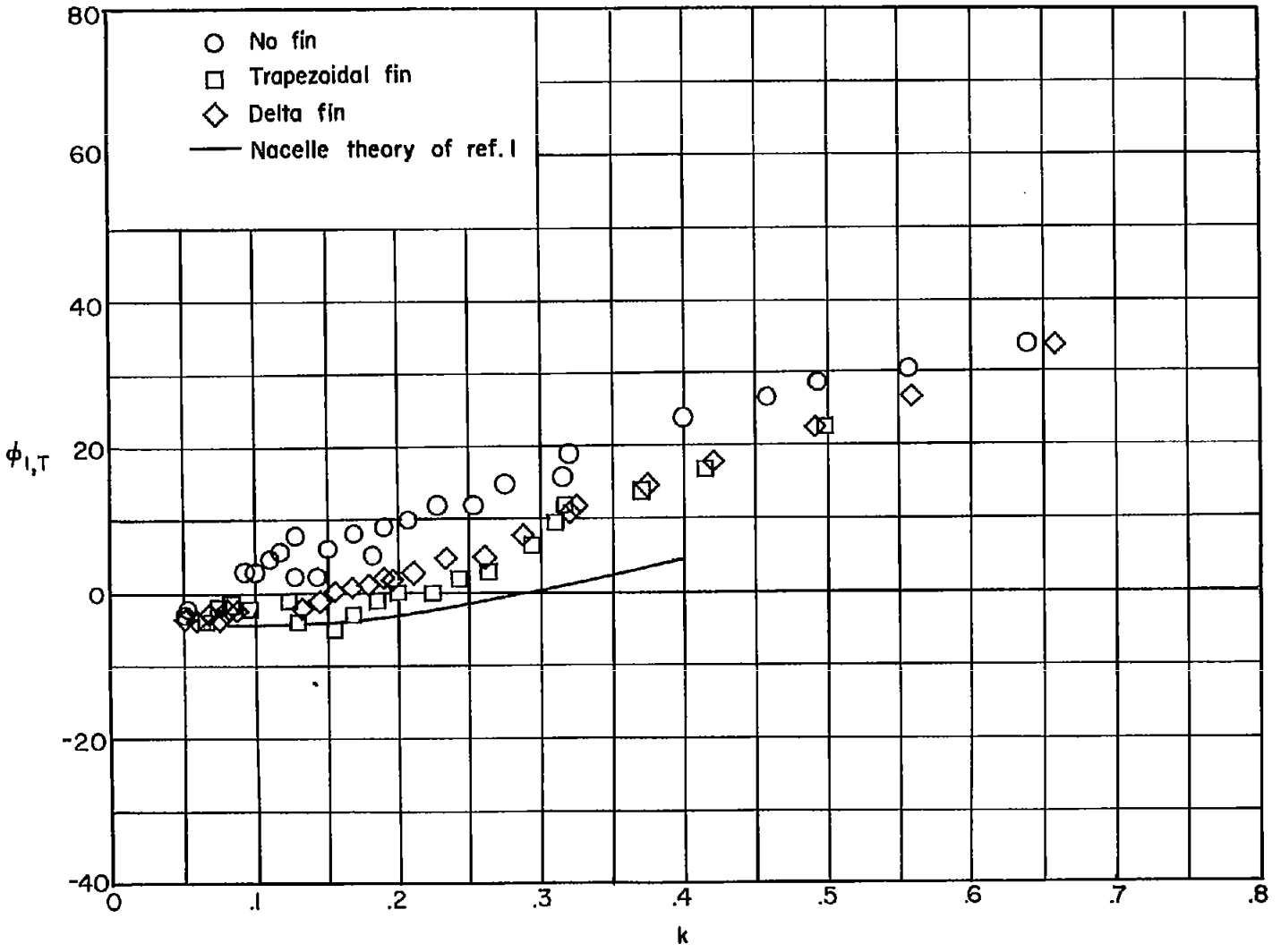

Figure 9.- Variation of experimental lift phase angle with reduced frequency for the oscillating tank.

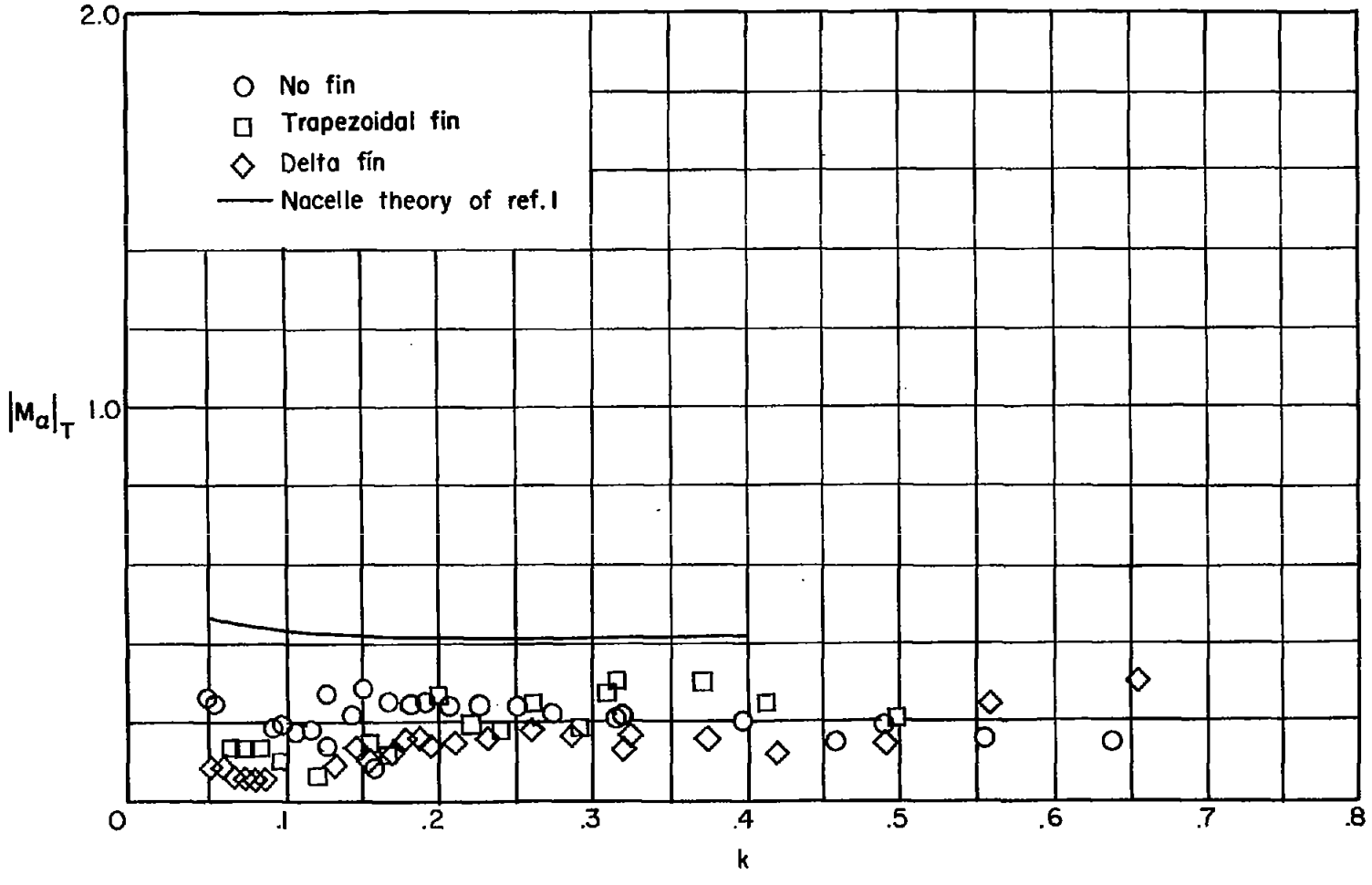

Figure 10.- Variation of experimental moment coefficient with reduced frequency for the oscillating tank.

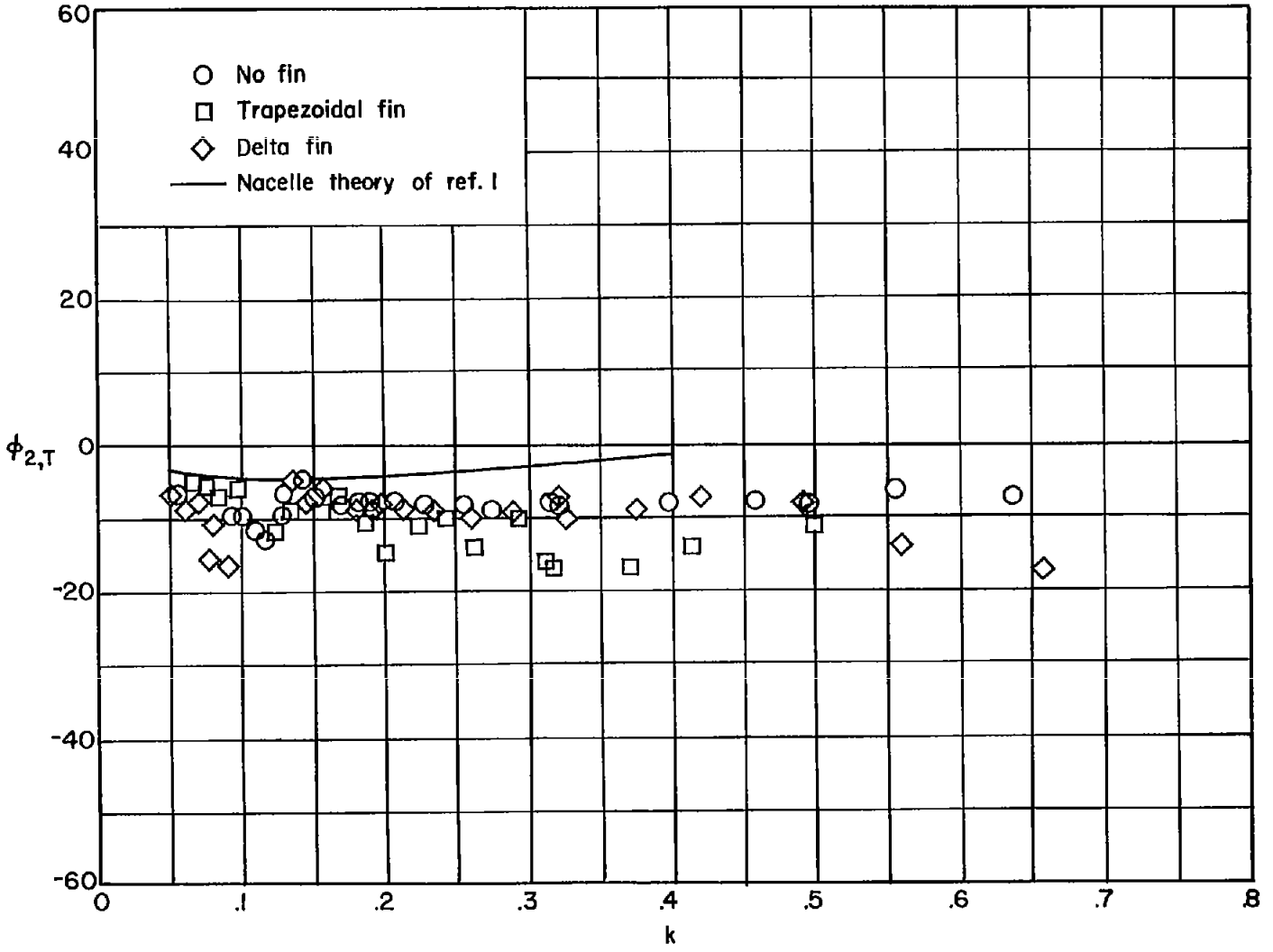

Figure 11.- Variation of experimental moment phase angle with reduced frequency for the oscillating tank.